

# The nuclear liquid–gas phase transition within Fermionic Molecular Dynamics

J. Schnack<sup>1</sup> and H. Feldmeier<sup>2</sup>

*Gesellschaft für Schwerionenforschung mbH,  
Postfach 110 552, D-64220 Darmstadt &  
Technische Hochschule Darmstadt*

---

## Abstract

The time evolution of excited nuclei, which are in equilibrium with the surrounding vapour, is investigated. It is shown that the finite nuclear systems undergo a first order phase transition. The caloric curve is presented for excited  $^{16}\text{O}$ ,  $^{24}\text{Mg}$ ,  $^{27}\text{Al}$  and  $^{40}\text{Ca}$  and the critical temperature is estimated for  $^{16}\text{O}$ .

*PACS:* 24.10.Cn, 02.70.Ns, 05.30.-d, 05.30.Fk, 05.60.+w, 05.70.Fh

*Keywords:* Fermion system; Fermionic Molecular Dynamics; Time averaging; Ergodic assumption; Nuclear liquid–gas phase transition; Critical temperature

---

## 1 Introduction

Mean–field models predict a first order phase transition for nuclear matter with a critical temperature which depends on the proton–neutron asymmetry [1–5]. A recent experimental attempt by the ALADIN group [6] to deduce an equation of state, which relates the excitation energy of a hot nucleus to its temperature, has stimulated both, theoretical and experimental efforts in this field [7–13]. In the experiment excited projectile spectators were investigated in Au+Au collisions at a beam energy of  $E/A = 600$  MeV. While the equation of state refers to a stationary system where liquid and vapour (evaporated nucleons) are in equilibrium, the experiment deals with an expanding source. This causes some uncertainties for the temperature, which is deduced from isotope ratios, since the system cools while it is expanding.

In molecular–dynamics calculations the finite system may be excited without flow, but similar problems arise when the phase transition sets in. Particles

---

<sup>1</sup> email: j.schnack@gsi.de, WWW: <http://www.gsi.de/~schnack>

<sup>2</sup> email: h.feldmeier@gsi.de, WWW: <http://www.gsi.de/~feldm>

which escape from the nucleus cool down the residue and thermal equilibrium cannot be maintained. In order to avoid these difficulties, in the present simulations the excited nuclear system is confined by a wide container potential which is chosen to be a harmonic oscillator potential. Its frequency  $\omega$  serves as a thermodynamic variable like the volume in the ideal gas case. Due to the containment evaporated nucleons cannot escape, but form a cloud of equilibrated vapour around the excited nucleus.

Thermodynamic relations are obtained by coupling the nuclear system to a reference system which serves as a thermometer. Both, the time–evolution of the nuclear system and of the thermometer are described by the Fermionic Molecular Dynamics (FMD) model. Assuming thermal equilibrium in the sense of ergodicity the temperature of the nuclear system is derived from the time–averaged energy of the thermometer and related to the excitation energy of the nucleus.

## 2 Model and setup

### 2.1 The Fermionic Molecular Dynamics model

The time evolution of the nuclear system is described within the framework of Fermionic Molecular Dynamics (FMD) published in detail in Ref. [14]. The model describes the many–body system with a parameterized antisymmetric many–body state  $|Q(t)\rangle$  composed of single–particle Gaussian wave packets

$$\langle \vec{x} | q(t) \rangle = \exp \left\{ -\frac{(\vec{x} - \vec{b}(t))^2}{2a(t)} \right\} \otimes |m_s\rangle \otimes |m_t\rangle, \quad (1)$$

$$\vec{b}(t) = \vec{r}(t) + i a(t) \vec{p}(t),$$

which are localized in phase space at  $\vec{r}$  and  $\vec{p}$  with a complex width  $a$ . Spin and isospin are chosen to be time–independent in these calculations; they are represented by their  $z$ –components  $m_s$  and  $m_t$ , respectively. Given the Hamilton operator  $\underline{H}$  the equations of motion for all parameters are derived from the time–dependent variational principle (operators are underlined with a tilde)

$$\delta \int_{t_1}^{t_2} dt \langle Q(t) | i \frac{d}{dt} - \underline{H} | Q(t) \rangle = 0. \quad (2)$$

In the present investigation the effective two-body nucleon–nucleon interaction  $\mathcal{V}$  in the Hamilton operator consists of a short-range repulsive and long-range attractive central potential with spin and isospin admixtures and includes the Coulomb potential [15]. The parameters of the interaction have been adjusted to minimize deviations between calculated and measured binding energies and charge radii for nuclei with mass numbers  $4 \leq A \leq 40$ .

## 2.2 The container

Besides the kinetic energy  $\mathcal{T}$  and the nucleon–nucleon interaction  $\mathcal{V}$  the Hamilton operator  $\mathcal{H}$  includes an external field

$$\mathcal{U}(\omega) = \frac{1}{2} m\omega^2 \sum_{i=1}^A \vec{x}_i^2 \quad (3)$$

which serves as a container.

The container is an important part of the setup because it keeps the evaporated nucleons (vapour) in the vicinity of the remaining liquid drop so that it equilibrates with the surrounding vapour. The vapour pressure is controlled by the external parameter  $\omega$ , which appoints the accessible volume.

## 2.3 The thermometer

The concept of determining the temperature is to bring a reference system, for which thermodynamic relations between temperature and measurable quantities are known, into thermal equilibrium with the investigated system. The weakly interacting ideal gas, where the temperature is given by the mean kinetic energy of the particles, may serve as an example. The reference system is called a heat bath if its heat capacity is much larger than that of the system and it is called a thermometer if its heat capacity is much less.

As the nuclear system is quantal and strongly interacting its temperature cannot be deduced from the momentum distribution or the mean kinetic energy of the nucleons. Therefore, the concept of an external thermometer which is coupled to the nuclear system is used in the present investigation. The thermometer consists of a quantum system of distinguishable particles moving in a common harmonic oscillator potential different from the container potential.

The time evolution of the whole system is described by the FMD equations of motion. For this purpose the many-body trial state is extended and contains

now both, the nucleonic degrees of freedom and the thermometer degrees of freedom

$$|Q\rangle = |Q_n\rangle \otimes |Q_{th}\rangle . \quad (4)$$

The total Hamilton operator including the thermometer is given by

$$\underline{H} = \underline{H}_n + \underline{H}_{th} + \underline{H}_{n-th} , \quad \underline{H}_n = \underline{T} + \underline{V} + \underline{U}(\omega) \quad (5)$$

with the nuclear Hamilton operator  $\underline{H}_n$  and the thermometer Hamilton operator

$$\underline{H}_{th} = \sum_{i=1}^{N_{th}} \left( \frac{\vec{k}^2(i)}{2 m_{th}(i)} + \frac{1}{2} m_{th}(i) \omega_{th}^2 \vec{x}^2(i) \right) . \quad (6)$$

The coupling between nucleons and thermometer particles,  $\underline{H}_{n-th}$ , is assumed to be weak, repulsive and of short range. It has to be as weak as possible in order not to influence the nuclear system too much. On the other hand it has to be strong enough to allow for reasonable equilibration times. Our choice is to put more emphasis on small correlation energies, smaller than the excitation energy, and to tolerate long equilibration times.

The determination of the caloric curve is done in the following way. The nucleus is excited by displacing all wave packets from their ground-state positions randomly. Both, centre of mass momentum and total angular momentum are kept fixed at zero. To allow a first equilibration between the wave-packets of the nucleus and those of the thermometer the system is evolved over a long time (10000 fm/c). After that a time-averaging of the energy of the nucleonic system as well as of the thermometer is performed over a time interval of 10000 fm/c. During this time interval the mean of the nucleonic excitation energy

$$E^* = \frac{1}{N_{steps}} \sum_{i=1}^{N_{steps}} \langle Q_n(t_i) | \underline{H}_n | Q_n(t_i) \rangle - E_0(N, Z) \quad (7)$$

is evaluated.  $E_0(N, Z)$  denotes the FMD ground-state energy of the isotope under consideration. The time-averaged energy of the thermometer  $E_{th}$ , which is calculated during the same time interval, determines the temperature  $T$  through the relation for an ideal gas of distinguishable particles in a common harmonic oscillator potential (Boltzmann statistics)

$$T = \hbar\omega_{th} \left[ \ln \left( \frac{E_{th}/N_{th} + \frac{3}{2}\hbar\omega_{th}}{E_{th}/N_{th} - \frac{3}{2}\hbar\omega_{th}} \right) \right]^{-1}. \quad (8)$$

### 3 The caloric curve

The relation between the excitation energy and the temperature is determined for the four nuclei  $^{16}\text{O}$ ,  $^{24}\text{Mg}$ ,  $^{27}\text{Al}$  and  $^{40}\text{Ca}$  using the same container potential with  $\hbar\omega = 1$  MeV. In addition the dependence on  $\omega$  is investigated for  $^{16}\text{O}$  leading to an estimate of the critical temperature.

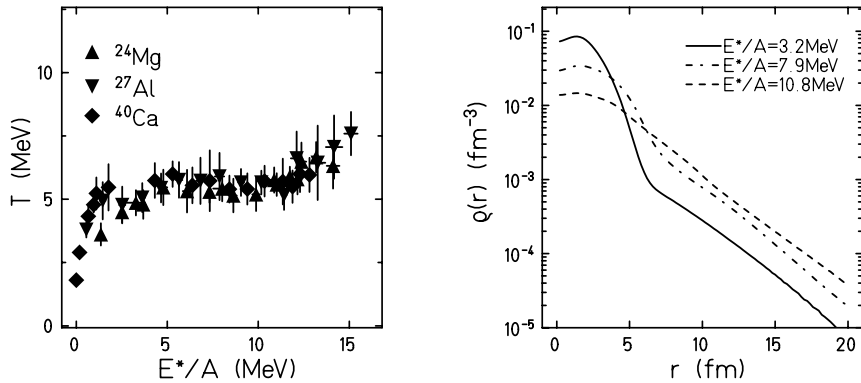


Fig. 1. L.h.s.: caloric curve of  $^{24}\text{Mg}$ ,  $^{27}\text{Al}$  and  $^{40}\text{Ca}$  at  $\hbar\omega = 1$  MeV, r.h.s.: time-averaged radial density distribution of  $^{24}\text{Mg}$  at various excitation energies in the coexistence region.

The caloric curve shown in the graph on the left hand side of fig. 1 clearly exhibits three different parts. Beginning at small excitation energies the temperature rises steeply with increasing energy as expected for the shell model. The nucleons remain bound in the excited nucleus which behaves like a drop of liquid. At an excitation energy of 3 MeV per nucleon the curve flattens and stays almost constant up to about 11 MeV. This plateau at  $T \approx 5$  MeV has its origin in the coexistence of liquid and vapour phases, the latter consisting of evaporated nucleons which are in equilibrium with the residual liquid drop due to the containment. At the beginning of the plateau the system contains only few evaporated nucleons, towards the end more and also small intermittent condensed fragments which may amalgamate or dissolve into vapour again. Around  $E^*/A \approx 11$  MeV all nucleons are unbound and the system has reached the vapour phase. This is reflected by the rise of the caloric curve beyond this point. The "error bars" denote the r.m.s. fluctuations in temperature and excitation energy, respectively, which arise from the energy exchange between thermometer and nucleons. Only the total energy of the system (nucleons & thermometer) is conserved. The magnitude of the temperature fluctuations is larger than those of  $E^*/A$  because the heat capacity of the thermometer is

smaller than that of the nucleus.

One has to keep in mind that the plateau, which due to finite size effects is rounded, is not the result of a Maxwell construction as in nuclear matter calculations. In the excitation energy range between 3 and 11 MeV per particle an increasing number of nucleons is found in the vapour phase outside the liquid phase. This can be seen in the density plot on the right hand side of figure 1, where the radial dependence of the time-averaged density of a system of 24 nucleons is shown at three excitation energies in the coexistence region. For small excitations ( $E^*/A = 3.2$  MeV) the nucleus, which is bouncing around due to recoil, is surrounded with very low density vapour (solid line). The dashed-dotted line ( $E^*/A = 7.9$  MeV) and the dashed line ( $E^*/A = 10.8$  MeV) show that with increasing energy the vapour contribution is growing and the amount of liquid decreasing. However, in the high energy part of the plateau the averaged one-body density displayed here does not represent the physical situation adequately. The time-dependent many-body state shows the formation and disintegration of several small drops. Above  $E^*/A \approx 13$  MeV only vapour is observed.

The caloric curve shown in fig. 1 has a striking similarity with the caloric curve determined by the ALADIN group [6] which is displayed in fig. 2. The position and the extension of the plateau agree with the FMD calculation using a containing oscillator potential of  $\hbar\omega = 1$  MeV. Nevertheless, there are important differences. The measurement addresses an expanding non-equilibrium system, but the calculation deals with a contained equilibrium system. In addition the used thermometers differ; the experiment employs an isotope thermometer based on chemical equilibrium and the calculation uses an ideal gas thermometer. One explanation why the thermodynamic description of the experimental situation works and compares nicely to the equilibrium result might be, that the excited spectator matter equilibrates faster into the coexistence region [16] than it expands and cools. The assumption of such a transient equilibrium situation [10,17,18] seems to work rather well at least in the plateau region. Further investigations on the FMD time evolution of excited nuclei without container will focus on such assumptions.

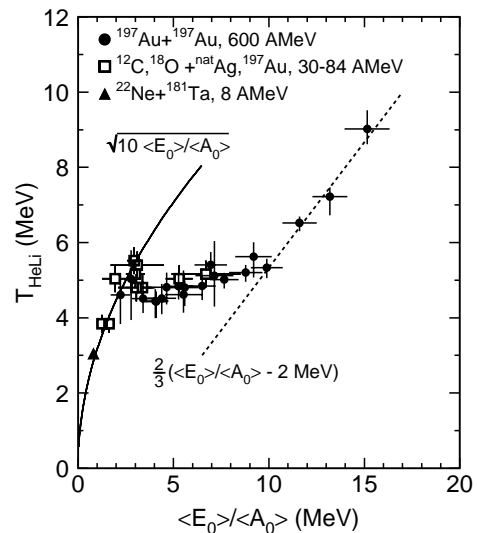


Fig. 2. Caloric Curve determined by the ALADIN group [6].

The thermodynamic properties of the nucleonic system are controlled by the

external parameter  $\omega$  similar to the volume in the case of an ideal gas. An increasing  $\omega$  leads to smaller volume and to higher pressure in the container which shifts the plateau of the caloric curve to higher temperatures and decreases its extension, i.e. the latent heat. The critical temperature  $T_c$  is reached for the  $\omega_c$  at which the plateau vanishes. Figure 3 displays this dependence for  $^{16}\text{O}$ . The caloric curve is evaluated for three different oscillator frequencies of the container potential. A pronounced plateau is seen in the plot on the left hand side, where the oscillator does not influence the self bound nucleus very much. In the middle part the more narrow container potential is already squeezing the ground state, its energy goes up to  $E/A \approx -5$  MeV. The plateau is shifted to  $T \approx 7$  MeV and the latent heat is decreased. On the right hand side, for  $\hbar\omega = 18$  MeV, the coexistence region has almost vanished. In addition one observes very large fluctuations of  $T$  and  $E$ .

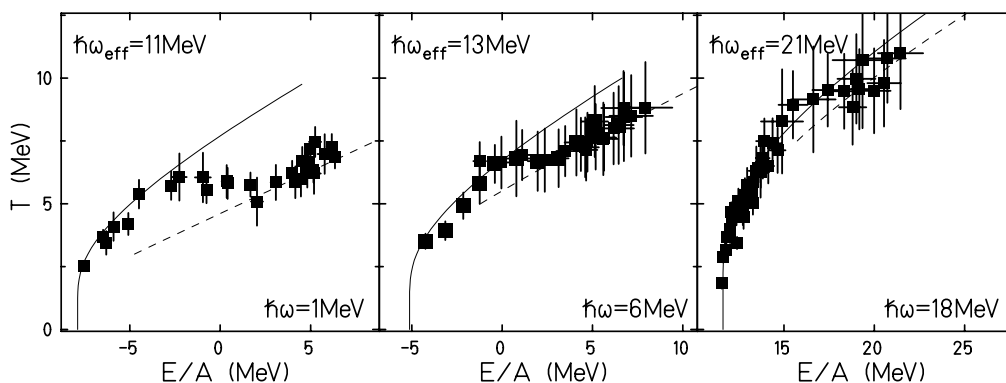


Fig. 3. Caloric curve of  $^{16}\text{O}$  for the frequencies  $\hbar\omega = 1, 6, 18$  MeV of the container potential. The solid lines show the low temperature behaviour of an ideal gas of 16 fermions in a common harmonic oscillator with level spacing  $\hbar\omega_{\text{eff}}$ , the dashed lines denote their high temperature behaviour in the confining oscillator ( $\hbar\omega$ ).

The critical temperature  $T_c$ , which can be estimated from the disappearance of the coexistence phase in figure 3, is about 10 MeV and has to be compared to the results of ref. [1,3,19] for finite nuclei including Coulomb and surface effects. All authors report a weak dependence of the critical temperature on the mass number in the region from calcium to lead. The result of Jaqaman et al. with the Skyrme ZR3 interaction [1] can be extrapolated to  $^{16}\text{O}$  to give  $T_c \approx 8$  MeV, Bonche et al. [3] arrive at the same number using the SKM interaction, but get  $T_c \approx 11$  MeV with the SIII interaction. Close to the last result is the value extrapolated from ref. [19] where  $T_c \approx 11.5$  MeV for Gogny's D1 interaction.

## Acknowledgments

The authors would like to thank the INT at the University of Washing-

ton/Seattle for the warm hospitality and G. Bertsch for stimulating discussions. This work was supported by a grant of the CUSANUSWERK to J. S..

## References

- [1] H.R. Jaqaman, A.Z. Mekjian, L. Zamik, Phys. Rev. C **29** (1984) 2067
- [2] A.L. Goodman, J.I. Kapusta, A.Z. Mekjian, Phys. Rev. C **30** (1984) 851
- [3] P. Bonche, S. Levit, D. Vautherin, Nucl. Phys. **A427** (1984) 278 and Nucl. Phys. **A436** (1985) 265
- [4] B. Serot, J.D. Walecka, Adv. Nucl. Phys. **16** (1986)
- [5] M. Schönhofen et al., Nucl. Phys. **A504** (1989) 875
- [6] J. Pochodzalla et al., Phys. Rev. Lett. **75** (1995) 1040
- [7] J.B. Natowitz et al., Phys. Rev. C **52** (1995) R2322
- [8] H. Müller, B.D. Serot, Phys. Rev. C **52** (1995) 2072
- [9] L.G. Moretto et al., Phys. Rev. Lett. **76** (1996) 2822;  
J. Pochodzalla et al., Phys. Rev. Lett. **76** (1996) 2823
- [10] G. Papp, W. Nörenberg, APH Heavy Ion Physics 1 (1995) 241
- [11] P. Finocchiaro, M. Belkacem, T. Kubo, V. Latora, A. Bonasera, Nucl. Phys. **A600** (1996) 236
- [12] J. Pochodzalla et al., Proceedings of the first Catania Relativistic Heavy Ion Studies, Acicastello (1996)
- [13] H. Xi, W.G. Lynch, M.B. Tsang, W.A. Friedman, Phys. Rev. **C54** (1996) R2163; M.B. Tsang, W.G. Lynch, H. Xi, W.A. Friedman, preprint, MSUCL-1035 (1996); H. Xi et al., preprint, MSUCL-1055 (1997)
- [14] H. Feldmeier, Nucl. Phys. **A515** (1990) 147; H. Feldmeier, K. Bieler, J. Schnack, Nucl. Phys. **A586** (1995) 493; H. Feldmeier, J. Schnack, Nucl. Phys. **A583** (1995) 347; J. Schnack, H. Feldmeier, Nucl. Phys. **A601** (1996) 181; H. Feldmeier, J. Schnack, Prog. Part. Nucl. Phys. **39** (1997)
- [15] J. Schnack, PhD thesis, TH Darmstadt (1996)
- [16] H. Feldmeier, J. Schnack, to be published in Advances in Nuclear Dynamics 3, Proceedings of 13th Winter Workshop on Nuclear Dynamics, edited by W. Bauer and A. Mignerey, Plenum Press (1997)
- [17] J.P. Bondorf, R. Donangelo, I.N. Mishustin, C.J. Pethick, H. Schulz, K. Sneppen, Nucl. Phys. **A443** (1985) 321
- [18] D.H.E. Gross, Rep. Prog. Phys. **53** (1990) 605 and references therein
- [19] Fu-guang Cao, Shan-de Yang, preprint, nucl-th/9612022